Charging in the Abrikosov lattice of type-II superconductors

Marie Ohuchi, Hikaru Ueki, 1,2 and Takafumi Kita 1 1 Department of Physics, Hokkaido University, Sapporo, Hokkaido 060-0810, Japan 2 Department of Mathematics and Physics, Hirosaki University, Hirosaki, Aomori 036-8561, Japan (Dated: April 9, 2021)

We study the temperature and magnetic field dependence of the vortex-core charge in the Abrikosov lattice of an s-wave superconductor based on the augmented quasiclassical equations with the Lorentz force and the pair-potential gradient (PPG) force. It is shown that the charging is dominated by the PPG force at weak magnetic fields and by the Lorentz force at strong magnetic fields, since the charge due to the PPG force, which is large at weak magnetic fields, decreases monotonically as the magnetic field increases, and that due to the Lorentz force has a large peak for the average of the flux density \bar{B} near $B_{c2}/2$, where B_{c2} is the upper critical field. Moreover, we estimate the magnitude of the vortex-core charge using the parameters used for cuprate superconductors, and found good agreement between our theoretical predictions and the NMR/NQR measurements by Kumagai et al. We show that the vortex-core charge peaks near T=0 and $\bar{B}=B_{c2}/2$, which makes it the most suitable region for a measurement of the charge.

I. INTRODUCTION

It is known that vortices in type-II superconductors have not only a single magnetic flux quantum but also accumulated charge. This vortex-core charging has attracted the interest of many researchers, and this has led to numerous theoretical studies. The earliest studies on the vortex-core charging were carried out based on the phenomenological theory [1-3] and the Bogoliubovde Gennes (BdG) equations [4-6]. London included the Lorentz force acting on supercurrents in his phenomenological equation, which provides a transparent way to show the existence of the vortex-core charge due to the Lorentz force acting on circulating supercurrents [1, 7]. Khomskii and Freimuth also calculated the vortex-core charge due to the chemical potential difference between the vortex-core region in the normal state and its surrounding region in the superconducting state by adopting the pair potential in the form of the step function [2, 8]. Matsumoto and Heeb first performed a selfconsistent calculation based on the BdG equations, including Maxwell's equations, in order to calculate the vortex-core charging in a chiral p-wave superconductor [5]. The vortex-core charging in a chiral p-wave superconductor was also calculated by using the Ginzburg-Landau Lagrangian with the Chern-Simons term [9]. Moreover, the dynamical dipole charge in the vortex core in type-II superconductors under an AC electromagnetic field was calculated by Eschrig et al. [10, 11]. It was also shown that the electric charge accumulates even at the vortex core of electrically neutral p-wave superfluids, although it is small compared with the core of superconductors [12]. Experimentally, the vortex-core charge in cuprate superconductors was estimated using the NMR/NQR measurements [13].

Recently, the augmented quasiclassical (AQC) equations of superconductivity with the three force terms were derived by incorporating the next-to-leading-order contributions in the expansion of the Gor'kov equations [14, 15] in terms of the quasiclassical parameter δ

 $1/k_{\rm F}\xi_0$ to study the vortex-core charging in type-II superconductors [16], where $k_{\rm F}$ is the amplitude of the Fermi wavenumber and $\xi_0 \equiv \hbar v_{\rm F}/\Delta_0$ is the coherence length with the energy gap Δ_0 at zero magnetic field and zero temperature, and the amplitude of the Fermi velocity $v_{\rm F}$. It has been elucidated that the vortex-core charging is caused by the three forces: (i) the Lorentz force that acts on supercurrents [1, 17, 18], (ii) pair-potential gradient (PPG) force [16, 19–21], and (iii) the pressure difference arising from the slope in the density of states (SDOS) [2, 8, 16]. In the isolated vortex system near the lower critical field, the vortex-core charge was calculated in swave superconductors with a cylindrical Fermi surface [21] and a spherical Fermi surface [16] based on the AQC equations with the three force terms. We found that the vortex-core charging in an s-wave superconductor with a spherical Fermi surface is dominated by the PPG force near zero temperature and by the SDOS pressure near the transition temperature when the magnetic penetration depth is larger than the coherence length, and the PPG force is dominant at low temperatures even if the magnetic penetration depth is almost the same as the coherence length [16]. Thus, the PPG force contributes dominantly to the vortex-core charge in a wide parameter range within the isolated vortex system. Masaki also studied the vortex-core charging in s- and chiral pwave superconductors with an isolated vortex based on the AQC equations with the Lorentz and PPG forces, and pointed out that the angular part coming from the phase of the pair potential in the PPG force contributes dominantly to the vortex-core charging [22]. The PPG force terms are divided into three parts: the radial part, which is the radial derivatives of the cylindrical coordinates around the vortex center, the angular part, which is the angular derivatives, and the vector potential terms coming from the gauge invariance of the AQC equations (See Eq. (6)). Therefore, the vortex-core charge is very small if the chirality and vorticity are antiparallel, i.e. $L_z = 0$, since the phase coming from each cancels out, where L_z is the total angular momentum. If the chirality

and vorticity are parallel, i.e. $L_z = 2$, the vortex-core charge is enhanced compared to that in s- and antiparallel chiral p-wave superconductors since a vortex has only the vorticity of $L_z = 1$ in s-wave superconductors. These results are consistent with those based on the BdG equations obtained by Matsumoto et al. [5]. The magnetic field dependence of the vortex-core charge was calculated in s-wave superconductors with a cylindrical Fermi surface [23] and in d-wave superconductors with anisotropic Fermi surfaces used for cuprates [24] based on the AQC equations with only the Lorentz force. It was shown that the charge density at the core has a large peak as a function of the magnetic field. On the other hand, to the best of our knowledge, the magnetic field dependence of the vortex-core charge due to the PPG force has not vet calculated. It is therefore worthwhile to calculate the field dependence of the charge due to the PPG force and compare it to that due to the Lorentz force.

The main purpose of this present paper is to develop a numerical method for calculating the temperature and magnetic field dependence of the vortex-core charge in the Abrikosov lattice [25] of type-II superconductors microscopically within the AQC equations with both the Lorentz and PPG forces, to shed more light on the mechanism of charging in the Abrikosov lattice, and to clarify the temperature and magnetic field dependence of the vortex-core charge in this mixed state. To this end, we calculate the temperature and magnetic field dependence of the vortex-core charge in a two-dimensional s-wave superconductor due to the Lorentz and PPG forces using the AQC equations of superconductivity in the Matsubara formalism. The SDOS pressure terms can be neglected in the case of superconductors with a cylindrical Fermi surface [21]. A recently used method may be more useful, but this formulation still only incorporates the Lorentz force [26]. We here perform the numerical calculation of the vortex-core charging combining the methods in Refs. [21] and [23].

This paper is organized as follows. In Sect. II, we present the formalism based on the AQC equations with the Lorentz and PPG forces in the Matsubara formalism, and show that the PPG force can be neglected in homogeneous superconductors. In Sect. III, we give numerical results for the charging in the vortex lattice of an s-wave superconductor with a cylindrical Fermi surface, and discuss the vortex-core charging due to the Lorentz and PPG forces. In Sect. IV, we provide a conclusion.

II. FORMALISM

A. Augmented quasiclassical equations

For clean s-wave superconductors in equilibrium, the AQC equations with the PPG and Lorentz forces in the

Matsubara formalism are given by [16, 21]

$$\begin{aligned} \left[i\varepsilon_{n}\hat{\tau}_{3} - \hat{\Delta}\hat{\tau}_{3}, \hat{g} \right] + i\hbar\boldsymbol{v}_{F} \cdot \boldsymbol{\partial}\hat{g} \\ + \frac{i\hbar}{2}e(\boldsymbol{v}_{F} \times \boldsymbol{B}) \cdot \frac{\partial}{\partial\boldsymbol{p}_{F}} \left\{ \hat{\tau}_{3}, \hat{g} \right\} \\ - \frac{i\hbar}{2}\boldsymbol{\partial}\hat{\Delta}\hat{\tau}_{3} \cdot \frac{\partial\hat{g}}{\partial\boldsymbol{p}_{F}} - \frac{i\hbar}{2}\frac{\partial\hat{g}}{\partial\boldsymbol{p}_{F}} \cdot \boldsymbol{\partial}\hat{\Delta}\hat{\tau}_{3} = \hat{0}, \quad (1) \end{aligned}$$

where $\hat{g} = \hat{g}(\varepsilon_n, p_{\rm F}, r)$ and $\hat{\Delta} = \hat{\Delta}(r)$ are the quasiclassical Green's functions and the pair potential, respectively, $\varepsilon_n = (2n+1)\pi k_{\rm B}T$ is the fermion Matsubara energy $(n=0,\pm 1,\cdots)$ with $k_{\rm B}$ and T denoting the Boltzmann constant and temperature, respectively, $v_{\rm F}$ and $p_{\rm F}$ are the Fermi velocity and momentum, respectively, e<0 is the electron charge, B=B(r) is the magnetic-flux density, the commutators are given by $[\hat{a},\hat{b}]\equiv \hat{a}\hat{b}-\hat{b}\hat{a}$, and $\{\hat{a},\hat{b}\}\equiv \hat{a}\hat{b}+\hat{b}\hat{a}$, and ∂ is the gauge-invariant differential operator given by

$$\partial \equiv \begin{cases} \nabla & \text{on } g \text{ or } \bar{g} \\ \nabla - i \frac{2e\mathbf{A}}{\hbar} & \text{on } f \text{ or } \Delta \\ \nabla + i \frac{2e\mathbf{A}}{\hbar} & \text{on } \bar{f} \text{ or } \Delta^* \end{cases}$$
(2)

with $\boldsymbol{A}=\boldsymbol{A}(\boldsymbol{r})$ denoting the vector potential. The first line in Eq. (1) corresponds to the standard Eilenberger equations [27–30], the second line is the Lorentz force terms [17, 18], and the third line is the PPG force terms [16, 20, 21]. We also assume spin-singlet pairing without spin paramagnetism. The matrices \hat{g} , $\hat{\Delta}$ and $\hat{\tau}_3$ are then expressible as [28]

$$\hat{g} = \begin{bmatrix} g & -if \\ i\bar{f} & -\bar{g} \end{bmatrix}, \quad \hat{\Delta} = \begin{bmatrix} 0 & \Delta \\ \Delta^* & 0 \end{bmatrix}, \quad \hat{\tau}_3 = \begin{bmatrix} 1 & 0 \\ 0 & -1 \end{bmatrix}, \quad (3)$$

where the barred functions are defined generally by $\bar{X}(\varepsilon_n, \mathbf{p}_{\mathrm{F}}, \mathbf{r}) \equiv X^*(\varepsilon_n, -\mathbf{p}_{\mathrm{F}}, \mathbf{r}).$

Following the procedure used in Ref. [7], we expand g and f formally in terms of $\delta \equiv 1/k_{\rm F}\xi_0$ as $g=g_0+g_1+\cdots$ and $f=f_0+f_1+\cdots$, where g_0 and f_0 are the solutions of the standard Eilenberger equations. The standard Eilenberger equations with the normalization condition $g_0 = \operatorname{sgn}(\varepsilon_n) \left(1 - f_0 \bar{f}_0\right)^{1/2}$ are given by [27–31]

$$\varepsilon_n f_0 + \frac{1}{2}\hbar \mathbf{v}_F \cdot \left(\mathbf{\nabla} - i\frac{2e\mathbf{A}}{\hbar}\right) f_0 = \Delta g_0,$$
 (4a)

$$\Delta = \Gamma_0 \pi k_{\rm B} T \sum_{n=-\infty}^{\infty} \langle f_0 \rangle_{\rm F}, \tag{4b}$$

$$\nabla \times \nabla \times \mathbf{A} = \mu_0 \mathbf{i}$$

$$\mathbf{j} = -i2\pi e N(0) k_{\rm B} T \sum_{n=-\infty}^{\infty} \langle \mathbf{v}_{\rm F} g_0 \rangle_{\rm F},$$
 (4c)

where j = j(r) is the current density, $\Gamma_0 \ll 1$ is the dimensionless coupling constant responsible for the Cooper

pairing, $\langle \cdots \rangle_{\rm F}$ is the Fermi surface average normalized as $\langle 1 \rangle_{\rm F} = 1$, μ_0 is the vacuum permeability, and N(0) is the normal density of states (DOS) per spin and unit volume at the Fermi energy. Equation (4) forms a set of self-consistent equations for f_0 , Δ , and A.

The equation for g_1 can be obtained from Eq. (1) as [16, 21]

$$v_{\rm F} \cdot \nabla g_1 = -e(v_{\rm F} \times \boldsymbol{B}) \cdot \frac{\partial g_0}{\partial \boldsymbol{p}_{\rm F}} - \frac{i}{2} \partial \Delta^* \cdot \frac{\partial f_0}{\partial \boldsymbol{p}_{\rm F}} - \frac{i}{2} \partial \Delta \cdot \frac{\partial \bar{f}_0}{\partial \boldsymbol{p}_{\rm F}}, \qquad (5)$$

with $g_1 = -\bar{g}_1$. Masaki called each terms including $(\partial \Delta/\partial r)\hat{r}$ and $(\partial \Delta/\partial \theta)(\hat{\theta}/r)$ in the PPG force $\partial \Delta$ the radial part and the angular part, respectively, which are defined by [22]

$$-\frac{i}{2}\frac{\partial \Delta^*}{\partial r}\hat{\boldsymbol{r}} \cdot \frac{\partial f_0}{\partial \boldsymbol{p}_{\mathrm{F}}} - \frac{i}{2}\frac{\partial \Delta}{\partial r}\hat{\boldsymbol{r}} \cdot \frac{\partial \bar{f}_0}{\partial \boldsymbol{p}_{\mathrm{F}}}, \quad \text{radial part}, \quad (6a)$$
$$-\frac{i}{2r}\frac{\partial \Delta^*}{\partial \theta}\hat{\boldsymbol{\theta}} \cdot \frac{\partial f_0}{\partial \boldsymbol{p}_{\mathrm{F}}} - \frac{i}{2r}\frac{\partial \Delta}{\partial \theta}\hat{\boldsymbol{\theta}} \cdot \frac{\partial \bar{f}_0}{\partial \boldsymbol{p}_{\mathrm{F}}}, \quad \text{angular part}.$$
(6b)

We also call the terms containing $-2ie\mathbf{A}\Delta/\hbar$, the vector potential terms, and are given by

$$\frac{e}{\hbar} \Delta^* \mathbf{A} \cdot \frac{\partial f_0}{\partial \mathbf{p}_{\mathrm{F}}} - \frac{e}{\hbar} \Delta \mathbf{A} \cdot \frac{\partial f_0}{\partial \mathbf{p}_{\mathrm{F}}}, \quad \text{vector potential terms,}$$
(6c)

where r and θ are the radius and the azimuth angle, respectively, in the cylindrical coordinate system $(r\cos\theta, r\sin\theta)$. The electric field $\mathbf{E} = \mathbf{E}(\mathbf{r})$ obeys [16]

$$-\lambda_{\mathrm{TF}}^{2} \nabla^{2} \mathbf{E} + \mathbf{E} = i \frac{\pi k_{\mathrm{B}} T}{e} \sum_{n=-\infty}^{\infty} \langle \nabla g_{1} \rangle_{\mathrm{F}}$$
$$-\frac{1}{e} \frac{N'(0)}{N(0)} \int_{-\tilde{\varepsilon}_{c}}^{\tilde{\varepsilon}_{c}} d\varepsilon \bar{n}(\varepsilon) \varepsilon \left\langle \nabla \mathrm{Re} g_{0}^{\mathrm{R}} \right\rangle_{\mathrm{F}} - \frac{c}{e} \frac{N'(0)}{N(0)} \nabla |\Delta|^{2}, \tag{7}$$

where $\lambda_{\rm TF} \equiv \sqrt{\epsilon_0 d/2e^2 N(0)}$ is the Thomas–Fermi screening length with ϵ_0 and d denoting the vacuum permittivity and the thickness, respectively [22, 32, 33], and the function $\bar{n}(\varepsilon) = 1/({\rm e}^{\varepsilon/k_{\rm B}T} + 1)$ is the Fermi distribution function for quasiparticles. The first term on the right-hand side of Eq. (7) comes from the Lorentz and PPG forces, while the second and third terms are the contributions from the SDOS pressure. The factor c first introduced by Khomskii et al.[2] is given by [16]

$$c \equiv \int_{-\tilde{\varepsilon}_c}^{\tilde{\varepsilon}_c} d\varepsilon \frac{1}{2\varepsilon} \tanh \frac{\varepsilon}{2k_{\rm B}T_{\rm c}},\tag{8}$$

where $T_{\rm c}$ is the superconducting transition temperature at zero magnetic field. The cutoff energies $\pm \tilde{\varepsilon}_{\rm c}$ are determined by [16]

$$\int_{-\tilde{\varepsilon}_{c}}^{\tilde{\varepsilon}_{c}} N_{s}(\varepsilon, \boldsymbol{r}) d\varepsilon = \int_{-\tilde{\varepsilon}_{c}}^{\tilde{\varepsilon}_{c}} N(\varepsilon) d\varepsilon, \quad N_{s}(\pm \tilde{\varepsilon}_{c}, \boldsymbol{r}) = N(\pm \tilde{\varepsilon}_{c}).$$
(9)

For example, as seen in Fig. 1 of Ref. [16], using the above condition for s-wave superconductors with a spherical Fermi surface, the superconducting DOS is connected to the normal DOS at the cutoff energies $\pm \tilde{\varepsilon}_{\rm c}$. Thus, the superconducting DOS becomes realistic and particle-hole asymmetric by including SDOS pressure terms. We again emphasize that we can neglect the SDOS pressure terms for superconductors with a cylindrical Fermi surface. These equations enable us to calculate the electric field and charge density microscopically.

B. Doppler shift method and homogeneous superconductors

Since the angular part, which originates from the phase of the pair potential in the PPG force terms, contributes dominantly to the charging in an isolated vortex of type-II superconductors [22], one may predict that the PPG force works even in superconductors with a constant energy gap, i.e. homogeneous superconductors, under magnetic fields, and causes the Hall effect near a surface. However, we show below that the PPG force does not work in homogeneous superconductors and within the Doppler shift method. To this end, we derive an expression for the Doppler shifted Green's functions and the Hall electric field in homogeneous superconductors by solving the AQC equations to study the action of the PPG force. We first express the pair potential and the anomalous Green's function as $\Delta(\mathbf{r}) = |\Delta(\mathbf{r})| e^{i\varphi(\mathbf{r})}$ and $f_0(\varepsilon_n, \mathbf{p}_F, \mathbf{r}) = \tilde{f}_0(\varepsilon_n, \mathbf{p}_F, \mathbf{r}) e^{i\varphi(\mathbf{r})}$, respectively, substitute them into Eq. (4a), and neglect the spatial derivative of \tilde{f}_0 . Then we obtain the Doppler-shifted Green's functions in the standard Eilenberger equations as

$$g_0 = \frac{\tilde{\varepsilon}_n}{\sqrt{\tilde{\varepsilon}_n^2 + |\Delta|^2}},\tag{10a}$$

$$\tilde{f}_0 = \frac{|\Delta|}{\sqrt{\tilde{\varepsilon}_p^2 + |\Delta|^2}},\tag{10b}$$

where $\tilde{\varepsilon}_n$ is defined by $\tilde{\varepsilon}_n \equiv \varepsilon_n + im \mathbf{v}_{\mathrm{F}} \cdot \mathbf{v}_{\mathrm{s}}$ with the superfluid velocity $\mathbf{v}_{\mathrm{s}} \equiv (\hbar/2m)(\nabla \varphi - 2e\mathbf{A}/\hbar)$ and the electron mass m. We also substitute Eq. (10) into Eq. (5) and then obtain

$$\mathbf{v}_{\mathrm{F}} \cdot \mathbf{\nabla} g_{1} = -e(\mathbf{v}_{\mathrm{F}} \times \mathbf{B}) \cdot \frac{\partial}{\partial \mathbf{p}_{\mathrm{F}}} \frac{\tilde{\varepsilon}_{n}}{\sqrt{\tilde{\varepsilon}_{n}^{2} + |\Delta|^{2}}}.$$
 (11)

Thus, the PPG force terms all cancel each other out, and we find that the PPG force does not work when $v_F \cdot \nabla \tilde{f}_0$ is zero. For example, when we consider an isolated vortex system, the Doppler shift method is an approximation that neglects the low energy excitations called the Carolide Gennes Matricon mode [34]. Therefore, the low energy excitations may be important for the PPG force to work.

We next assume that the gap amplitude is spatially constant as $|\Delta(\mathbf{r})| = |\Delta|$, and expand g_0 , f_0 , and $\mathbf{v}_F \cdot \nabla g_1$

up to the first-order in v_s as

$$g_0 = \frac{\varepsilon_n}{\sqrt{\varepsilon_n^2 + |\Delta|^2}} + im \mathbf{v}_F \cdot \mathbf{v}_s \frac{|\Delta|^2}{(\varepsilon_n^2 + |\Delta|^2)^{3/2}}, \quad (12a)$$

$$\tilde{f}_0 = \frac{|\Delta|}{\sqrt{\varepsilon_n^2 + |\Delta|^2}} - im \mathbf{v}_F \cdot \mathbf{v}_s \frac{\varepsilon_n |\Delta|}{(\varepsilon_n^2 + |\Delta|^2)^{3/2}}, \quad (12b)$$

 $\boldsymbol{v}_{\mathrm{F}}\cdot \boldsymbol{\nabla} g_1$

$$= -ie(\boldsymbol{v}_{\mathrm{F}} \times \boldsymbol{B}) \cdot \frac{\partial}{\partial \boldsymbol{p}_{\mathrm{F}}} m \boldsymbol{v}_{\mathrm{F}} \cdot \boldsymbol{v}_{\mathrm{s}} \frac{|\Delta|^{2}}{(\varepsilon_{n}^{2} + |\Delta|^{2})^{3/2}}. \quad (12c)$$

Substituting Eqs. (12a) and (12b) into Eqs. (4c) and (4b), respectively, and using $\langle v_F \rangle_F = 0$, we obtain the gap equation and the London equation as [28]

$$1 = 2\pi\Gamma_0 k_{\rm B} T \sum_{n=0}^{\infty} \left\langle \frac{1}{\sqrt{\varepsilon_n^2 + |\Delta|^2}} \right\rangle_{\rm F},\tag{13a}$$

$$\nabla^2 B = \frac{1}{\lambda_1^2} B,\tag{13b}$$

where $\lambda_{\rm L}$ is the London penetration depth at finite temperatures $\lambda_{\rm L} \equiv \lambda_0 [(2/3)(1-Y)]^{-1/2}, \ \lambda_0$ is the magnetic penetration depth $\lambda_0 \equiv \left[\mu_0 N(0) e^2 v_{\rm F}^2\right]^{-1/2}$, and Y=Y(T) is the Yosida function [7, 28, 35] defined by

$$Y \equiv 1 - 2\pi k_{\rm B} T \sum_{n=0}^{\infty} \frac{|\Delta|^2}{(\varepsilon_n^2 + |\Delta|^2)^{3/2}}.$$
 (14)

Furthermore, considering the region outside the vortex core or a surface without any spatial variation in the gap amplitude, substituting Eq. (12c) into Eq. (7), and using $g_1 = -\bar{g}_1$, the equation for the electric field in homogeneous superconductors is given by

$$-\lambda_{\mathrm{TF}}^{2} \nabla^{2} \boldsymbol{E} + \boldsymbol{E} = \boldsymbol{B} \times \underline{R}_{\mathrm{H}} \boldsymbol{j}, \qquad (15)$$

where $\underline{R}_{\rm H}$ is the equilibrium Hall coefficient tensor in homogeneous superconductors given by

$$\boldsymbol{j} = meN(0)(1 - Y)\langle \boldsymbol{v}_{\mathrm{F}} \boldsymbol{v}_{\mathrm{F}} \rangle_{\mathrm{F}} \boldsymbol{v}_{\mathrm{s}}, \tag{16a}$$

$$\underline{R}_{\mathrm{H}} = \frac{1}{2eN(0)} \left\langle \frac{\partial}{\partial \boldsymbol{p}_{\mathrm{F}}} \boldsymbol{v}_{\mathrm{F}} \right\rangle_{\mathrm{F}} \langle \boldsymbol{v}_{\mathrm{F}} \boldsymbol{v}_{\mathrm{F}} \rangle_{\mathrm{F}}^{-1}. \tag{16b}$$

This is the same as the result obtained in Ref. [7], despite taking into account the PPG force. Therefore, the Lorentz force works in homogeneous superconductors in the presence of magnetic fields, as calculated in the previous work [7], but the PPG force does not. We can also show that the PPG force does not work in anisotropic [33] and chiral [22] superconductors based on the corresponding AQC equations if $\mathbf{v}_{\mathrm{F}} \cdot \nabla \tilde{f}_{0}$ is zero. In the next section, we show that how the PPG force works in the vortex lattice as one example of when it is nonzero.

III. NUMERICAL RESULTS

A. Numerical procedures

We solve Eqs. (4), (5), and (7) numerically for a triangular vortex lattice of an s-wave type-II superconductor with a cylindrical Fermi surface based on the methods in Refs. [21] and [23]. We take the magnetic field to be along the axial direction of the cylinder. The corresponding vector potential is expressible in terms of the average flux density $\bar{B} = (0, 0, \bar{B})$ as $A(r) = (\bar{B} \times r)/2 + \tilde{A}(r)$, where \tilde{A} denotes the spatial variation of the flux density. Functions $\tilde{A}(r)$, E(r), and $\Delta(r)$ for the triangular lattice obey the following periodic boundary conditions [36–38]:

$$\tilde{A}(r+R) = \tilde{A}(r), \tag{17a}$$

$$E(r+R) = E(r), \tag{17b}$$

$$\Delta(\mathbf{r} + \mathbf{R}) = \Delta(\mathbf{r})e^{i\chi(\mathbf{r})},$$

$$\chi(\mathbf{r}) \equiv \frac{|e|}{\hbar} \bar{\mathbf{B}} \cdot (\mathbf{r} \times \mathbf{R})$$

$$+ \frac{|e|}{\hbar} \bar{\mathbf{B}} \times (\mathbf{a}_1 - \mathbf{a}_2) \cdot \mathbf{R} + \pi n_1 n_2, \qquad (17c)$$

where $\mathbf{R} = n_1 \mathbf{a}_1 + n_2 \mathbf{a}_2$ with the integers n_1 and n_2 , and $\mathbf{a}_1 = a_2(\sqrt{3}/2, 1/2, 0)$ and $\mathbf{a}_2 = a_2(0, 1, 0)$ are the basic vectors of the triangular lattice with the length a_2 determined by the flux-quantization condition $(\mathbf{a}_1 \times \mathbf{a}_2) \cdot \bar{\mathbf{B}} = h/2|e|$. The Green's functions also satisfy the periodic boundary conditions as

$$q_0(\varepsilon_n, \boldsymbol{p}_{\mathrm{F}}, \boldsymbol{r} + \boldsymbol{R}) = q_0(\varepsilon_n, \boldsymbol{p}_{\mathrm{F}}, \boldsymbol{r}),$$
 (18a)

$$g_1(\varepsilon_n, \mathbf{p}_F, \mathbf{r} + \mathbf{R}) = g_1(\varepsilon_n, \mathbf{p}_F, \mathbf{r}),$$
 (18b)

$$f_0(\varepsilon_n, \mathbf{p}_{\mathrm{F}}, \mathbf{r} + \mathbf{R}) = f_0(\varepsilon_n, \mathbf{p}_{\mathrm{F}}, \mathbf{r}) \mathrm{e}^{i\chi(\mathbf{r})},$$
 (18c)

We first solve the standard Eilenberger equations (4) self-consistently for the vortex lattice using the Riccati method [28, 39–41]. The solution is substituted into the right-hand side of Eq. (5), which is solved by using the standard Runge–Kutta method. We next obtain the electric field substituting the solution to Eq. (5) into Eq. (7) and solving Eq. (7), and then calculate the charge density ρ using Gauss' law $\rho = \epsilon_0 d\nabla \cdot \mathbf{E}$, numerically. The results presented below are for $\lambda_{\rm TF} = 0.03\xi_0$, $\lambda_0 = 5\xi_0$ and $\delta = 0.03$, where λ_0 is the magnetic penetration depth at zero temperature, defined by $\lambda_0 \equiv \left[\mu_0 N(0)e^2\langle v_{\rm F}^2\rangle_{\rm F}\right]^{-1/2}$. The magnetic flux density is normalized by using $B_{\rm c2} = \mu_0 H_{\rm c2}$ obtained from the Helfand–Werthamer theory [42, 43], where $H_{\rm c2}$ is the upper critical field.

B. Results

Fig. 1 plots the spatial variations of the gap amplitude $|\Delta(r)|$ and the z-component of the magnetic-flux density

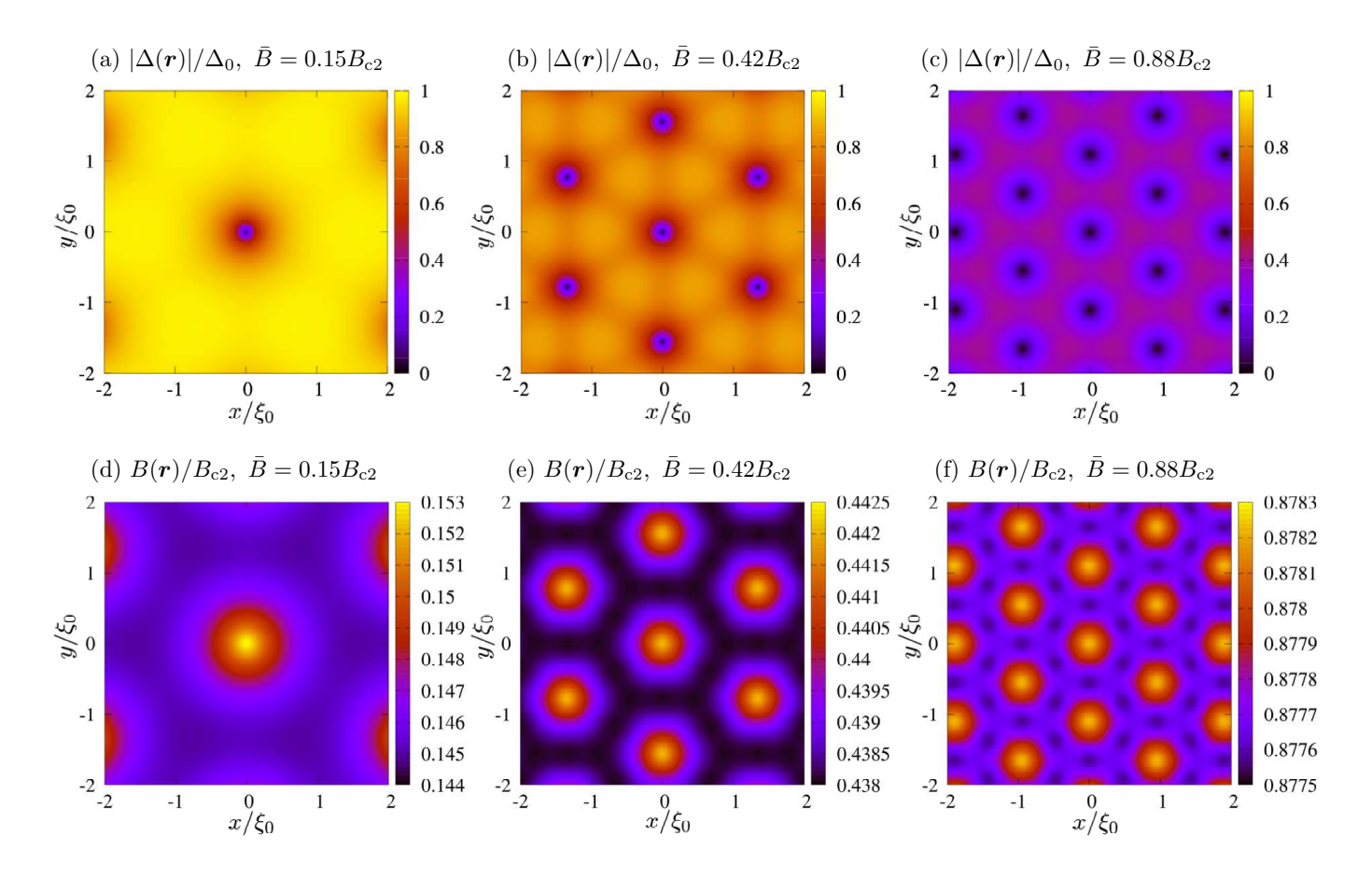


FIG. 1. Gap amplitude $|\Delta(\mathbf{r})|$ ((a), (b), and (c)) and the magnetic-flux density $B(\mathbf{r})$ ((d), (e), and (f)) at temperature $T = 0.2T_{\rm c}$ in units of the zero temperature gap Δ_0 and the upper critical field $B_{\rm c2}$ on a square grid with x and y ranging from $[-2\xi_0, +2\xi_0]$ for the average flux densities $\bar{B} = 0.15B_{\rm c2}$, $0.42B_{\rm c2}$, and $0.88B_{\rm c2}$ from left to right, respectively.

B(r), respectively, at temperature $T = 0.2T_c$ for the average flux densities $\bar{B} = 0.15B_{c2}$, $0.42B_{c2}$, and $0.88B_{c2}$, respectively. It is shown that the gap amplitude away from the vortex center and its slope at the vortex center become small together (See also Fig. 6), and the B/\bar{B} at vortex center is also small, i.e. the flux density becomes spatially uniform at strong magnetic fields compared with weak fields. We also find that the distance between two neighboring vortices becomes smaller and the angular dependence of the gap amplitude and flux density becomes larger when the vortex center is the origin at strong magnetic fields. Figure 2 shows the radial dependence of the gap amplitude and the magnetic-flux density around the core, respectively, at the azimuth angles $\theta = \pi/3$ and $\theta = \pi/2$ for temperature $T = 0.2T_c$ and the average flux densities $\bar{B} = 0.15B_{c2}$ and $0.88B_{c2}$, respectively. We can easily see this angular dependence by using Fig. 2. Thus, we have reproduced the earlier prediction by Ichioka et al. [38].

In Fig. 3, we show plots for the spatial dependence of the charge density due to the Lorentz force and the PPG force at temperature $T=0.2T_{\rm c}$ for the average flux densities $\bar{B}=0.15B_{\rm c2},~0.42B_{\rm c2},~{\rm and}~0.88B_{\rm c2},~{\rm respectively}.$ We see that the charges are accumulated at the core

where the pair potential is zero, and the accumulated charge due to the PPG force is larger at $\bar{B} = 0.15B_{\rm c2}$ and smaller at $B = 0.42B_{c2}$ and $0.88B_{c2}$, compared with that due to the Lorentz force. We will show a figure of the magnetic dependence of the charge density at the vortex center below in Fig. 5. We also find that a large charge accumulates at the midpoints between two neighboring vortices for $\bar{B} = 0.88B_{\rm c2}$ as the distance between vortices gets smaller. Figure 4 shows the current density j(r) at temperature $T=0.2T_{\rm c}$ for the average flux densities $\bar{B} = 0.15B_{c2}$, $0.42B_{c2}$, and $0.88B_{c2}$. The current density in the opposite direction to that around the core is created around the midpoints between the two neighboring vortices. Therefore, the negative charges accumulate at these midpoints due to the Lorentz force acting on the currents in the opposite direction to those around the core. On the other hand, it is difficult to explain the large negative charges due to the PPG force at these midpoints in Fig. 3(f) and the negatively charged lines connecting two neighboring vortices in Figs. 3(a), 3(b), 3(d), and 3(e) using the current density in Figs. 4(a) and 4(b), but these may be explained as follows. The gap amplitude is a little suppressed where the negative charge is accumulated as seen in Figs. 1(a), 1(b), and 1(c). The

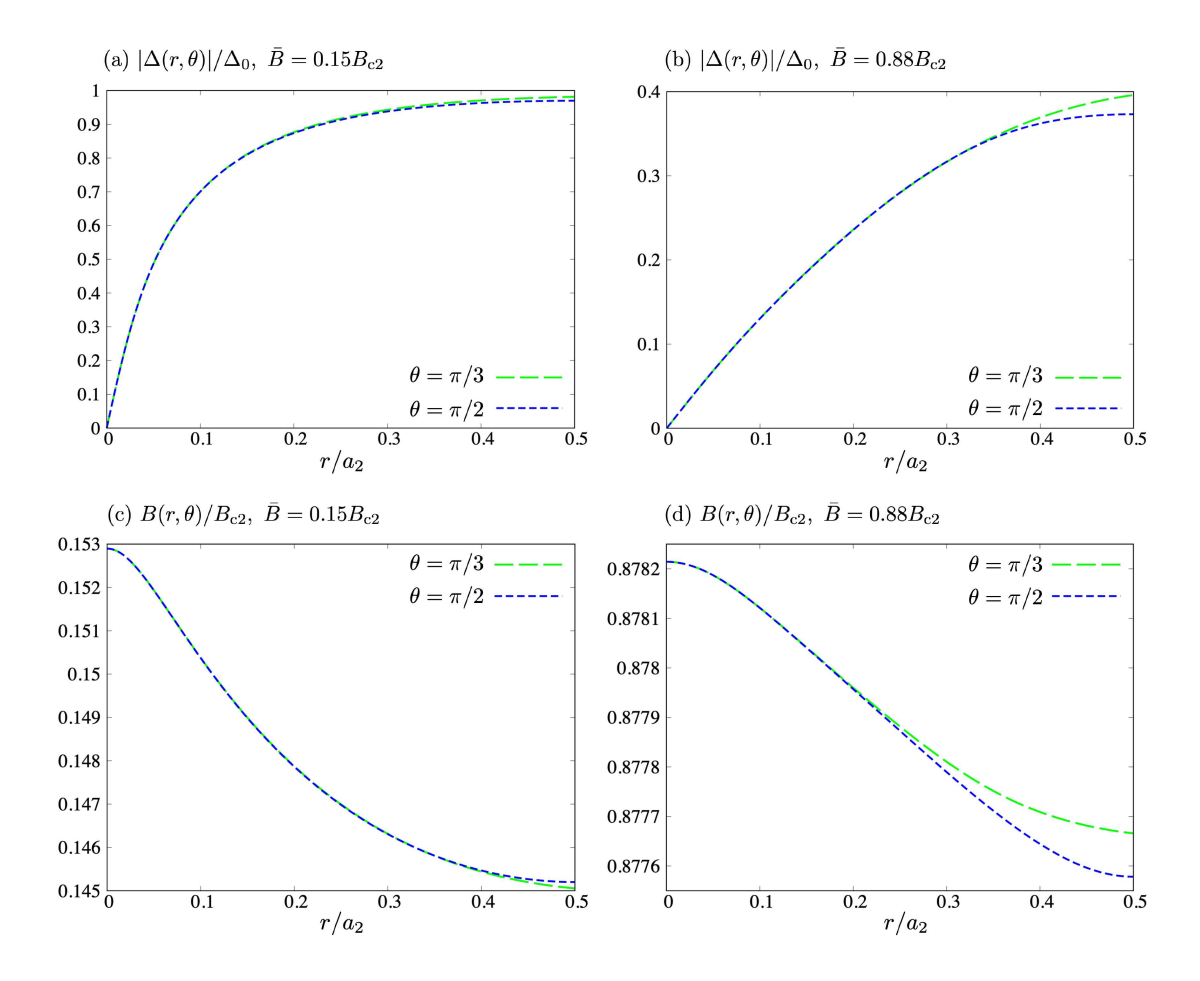


FIG. 2. Radial dependence of the gap amplitude $|\Delta(r,\theta)|$ ((a) and (b)) and the magnetic-flux density $B(r,\theta)$ ((c) and (d)) around the core at the azimuth angles $\theta = \pi/3$ (green dashed line) and $\theta = \pi/2$ (blue dotted line) in units of the zero temperature gap Δ_0 and the upper critical field B_{c2} over $0 \le r \le a_2$ for temperature $T = 0.2T_c$ and the average flux densities $\bar{B} = 0.15B_{c2}$ and $0.88B_{c2}$ from left to right, respectively.

charge density is more suppressed in the direction where the gap amplitude recovery is smaller as we move away from the core. Furthermore, considering the charge neutrality condition, the negative charges may accumulate there.

Fig. 5 shows the magnetic field dependence of the charge density at the vortex center due to the Lorentz force and the PPG force at temperatures $T=0.2T_{\rm c}$ and $T=0.5T_{\rm c}$, respectively. We confirm that the vortex-core charge due to the Lorentz force has a large peak of upper convexity as shown in the previous work [23]. However, the vortex-core charge due to the Lorentz force calculated by us is about 10 times larger than that calculated in the previous work [23], even if we use the same quasiclassical parameter. This is because the method in the previous work neglected the component perpendicular to the Fermi velocity of in ∇g_1 . We can explain that as follows. The equation for g_1 is obtained from the AQC

equations with only the Lorentz force as

$$\mathbf{v}_{\mathrm{F}} \cdot \mathbf{\nabla} g_1 = -e\mathbf{v}_{\mathrm{F}} \cdot \left(\mathbf{B} \times \frac{\partial g_0}{\partial \mathbf{p}_{\mathrm{F}}} \right).$$
 (19)

In the previous work, the above equation was approximated as

$$\nabla g_1 = -e \left(\mathbf{B} \times \frac{\partial g_0}{\partial \mathbf{p}_F} \right). \tag{20}$$

However, ∇g_1 may have a component perpendicular to $v_{\rm F}$. Therefore, we have here adopted a direct method for solving the equation for g_1 [Eq. (5)] in Refs. [16, 21]. We also confirm that the charge due to the PPG force at the core decrease monotonically with an increase in magnetic field. Figure 6 plots the gap amplitude $|\Delta(0,y)|$ and the x-component of the superfluid velocity $v_{\rm sx}(0,y)$ on the y-axis, for temperatures $T=0.2T_{\rm c}$ and the average flux densities $\bar{B}=0.15B_{\rm c2},~0.42B_{\rm c2},~{\rm and}~0.88B_{\rm c2},~{\rm and}~{\rm for}$ temperature $0.5T_{\rm c}$ and the average flux densities $\bar{B}=0.19B_{\rm c2},~0.58B_{\rm c2},~{\rm and}~0.87B_{\rm c2},~{\rm respectively}.$ The PPG

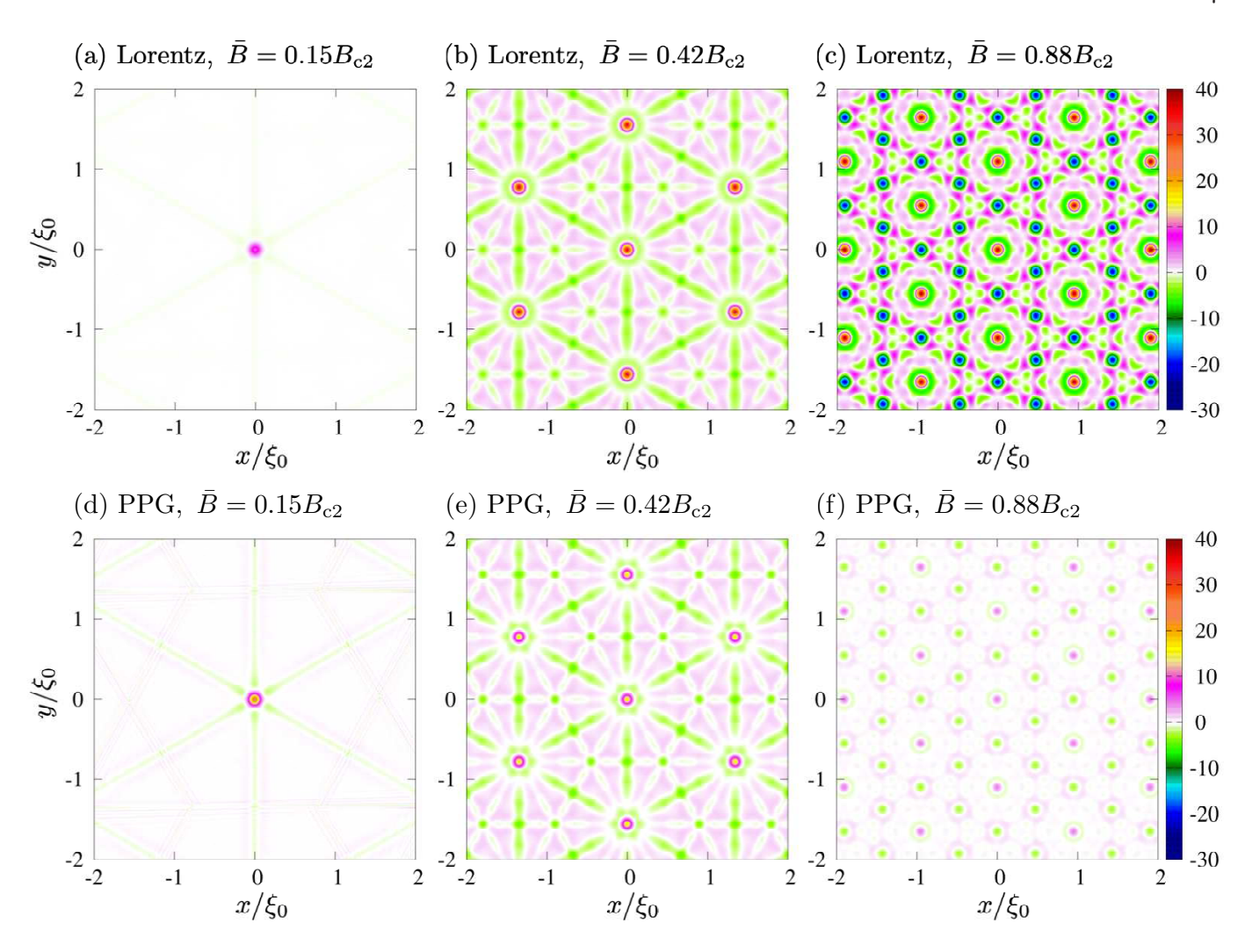


FIG. 3. Charge density $\rho(r)$ due to the Lorentz force ((a), (b), and (c)), and the PPG force ((d), (e), and (f)) at temperature $T=0.2T_{\rm c}$ in units of $\rho_0\equiv\Delta_0\epsilon_0d/|e|\xi_0^2$ on a square grid with x and y ranging from $[-2\xi_0,+2\xi_0]$ for the average flux densities $\bar{B}=0.15B_{\rm c2},~0.42B_{\rm c2},~{\rm and}~0.88B_{\rm c2}$ from left to right, respectively.

force terms in the g_1 equation [Eq. (5)] can be written as

$$-\frac{i}{2}\nabla|\Delta| \cdot \frac{\partial \tilde{f}_{0}}{\partial \boldsymbol{p}_{F}} - \frac{i}{2}\nabla|\Delta| \cdot \frac{\partial \tilde{f}_{0}}{\partial \boldsymbol{p}_{F}} + \frac{m}{\hbar}|\Delta|\boldsymbol{v}_{s} \cdot \frac{\partial \tilde{f}_{0}}{\partial \boldsymbol{p}_{F}} - \frac{m}{\hbar}|\Delta|\boldsymbol{v}_{s} \cdot \frac{\partial \tilde{f}_{0}}{\partial \boldsymbol{p}_{F}}.$$
 (21)

We here note that the definition of f_0 is written before Eq. (10). We can also confirm by numerical calculations that the first line in Eq. (21) is negligible, while the second line, which is the phase part, is dominant. Therefore, the charge decreases along with $|\Delta|$ as the magnetic field increases although v_s around the vortex center remains almost invariant. On the other hand, the charge due to the Lorentz force has a peak, coming from the competition between the increasing magnetic field and the decreasing pair potential [23]. Thus, the charge due to the PPG force without an explicit magnetic field behaves

differently from that due to the Lorentz force. Since the charges due to the PPG force and the Lorentz force are dominant at weak fields and at strong fields, respectively, the large charges are observed in a wide range of magnetic fields, although the peak of the charge appears near half the upper critical field. We also find that the vortex-core charge at $T=0.5T_{\rm c}$ is smaller than that at $T=0.2T_{\rm c}$ in all magnetic field regions. Moreover, since the upper critical field becomes lower as the temperature increases, the region where the PPG force becomes dominant also becomes relatively wider. Therefore, it is the best that measurements are performed at low temperatures and about half the upper critical field to detect the vortex-core charge experimentally.

To compare our result with the vortex-core charge estimated by the NMR/NQR measurements [13], we next calculate the order of magnitude for the accumulated charge around a vortex. We here adopt the core region of radius $0.2\xi_0$ and the thickness d=10 Å to roughly

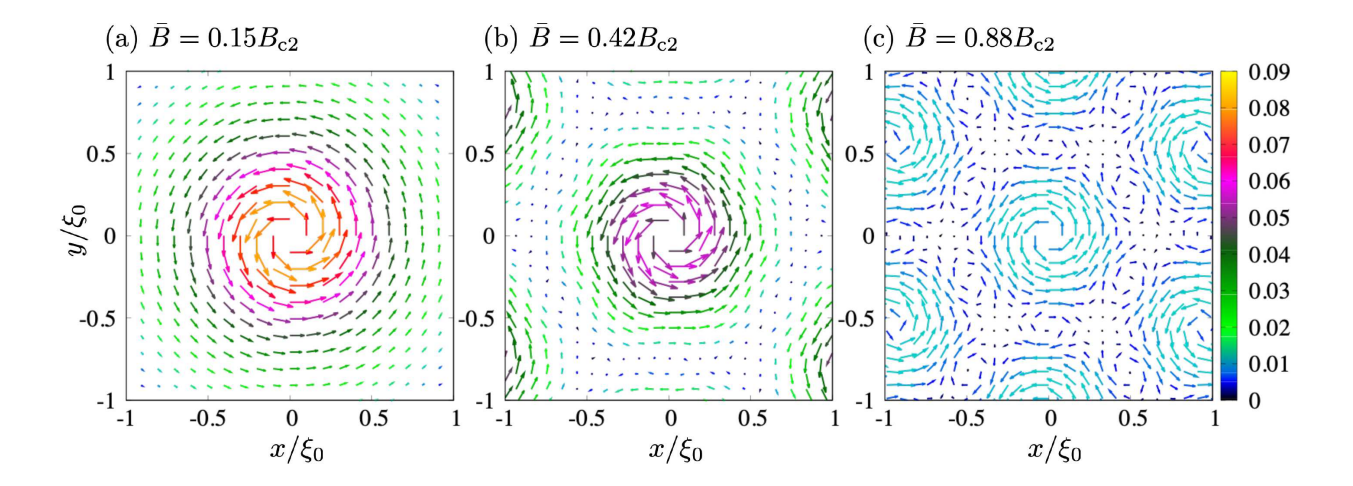


FIG. 4. Current density j(r) at temperature $T = 0.2T_c$ in units of $j_0 \equiv \hbar/2\mu_0 |e|\xi_0^3$ on a square grid with x and y ranging from $[-\xi_0, +\xi_0]$ or the average flux densities (a) $\bar{B} = 0.15B_{c2}$, (b) $0.42B_{c2}$, and (c) $0.88B_{c2}$ from left to right. The color bar indicates the magnitude of the current density and the length of the arrow does not.

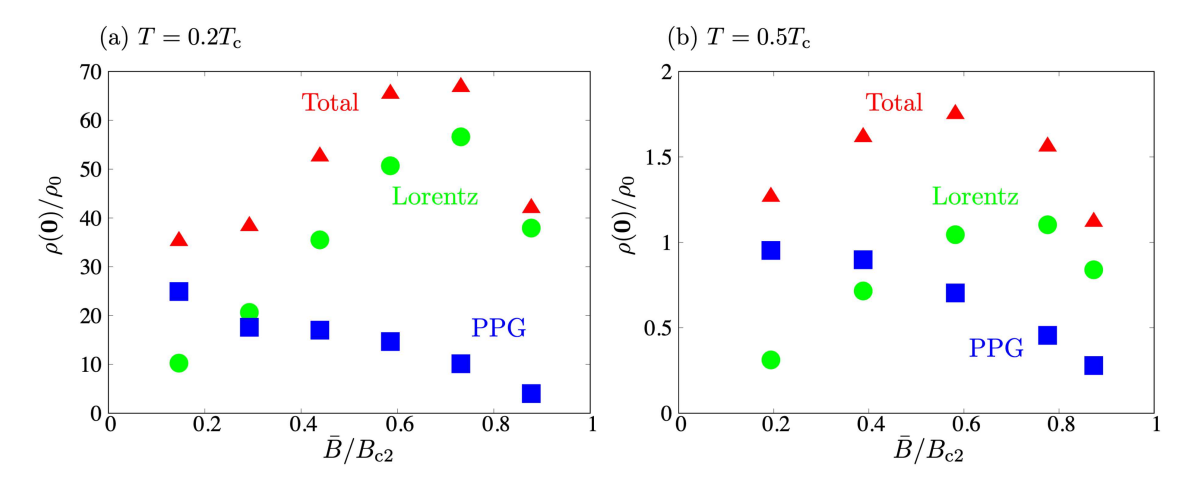


FIG. 5. Charge density at the vortex center $\rho(\mathbf{0})$ due to the Lorentz force (green circular points), the PPG force (blue square points), and the total force (red triangular points), in units of $\rho_0 \equiv \Delta_0 \epsilon_0 d/|e|\xi_0^2$ as a function of the magnetic field, at temperatures (a) $T = 0.2T_c$ and (b) $0.5T_c$ from left to right.

estimate the peak value of the accumulated charge Q. The vortex-core charge in YBCO at $T = 0.2T_c$ and $B = 0.73B_{\rm c2}$ is given by $Q \sim 10^{-3}|e|$ for the following appropriate parameters: $k_{\rm F}^{-1} \simeq 1.0$ Å, $\Delta_0 \simeq 28$ meV [44], and $\xi_0 \simeq 30$ Å [13]. The amount of charge estimated based on our present calculation is an order of magnitude larger than the charge reported in Ref. [23], owing to the difference in the calculation method as described above. The order of magnitude of the estimated charge in YBCO is roughly consistent with the experimental results by Kumagai et al. [13]. Although we note that while we calculate the vortex-core charge in s-wave superconductors, Kumagai et al. measured it in d-wave samples. In the case of unconventional superconductors, the spatial dependence of quantities near the vortex core is complicated by reflecting the anisotropic symmetry of those gaps [18]. On the other hand, we expect that the anisotropy of the gaps does not affect the charge magnitude in the core as much, but need to study that in more detail by solving the AQC equations.

IV. CONCLUSION

We have developed a numerical method for the study of charging in the vortex lattice state of type-II superconductors based on the AQC equations with the Lorentz and PPG forces. Using it, we have calculated the charge distribution in the vortex lattice of s-wave superconductors with a cylindrical Fermi surface. We have shown that the vortex-core charge in the Abrikosov lattice is dominated by the PPG force near the lower critical field

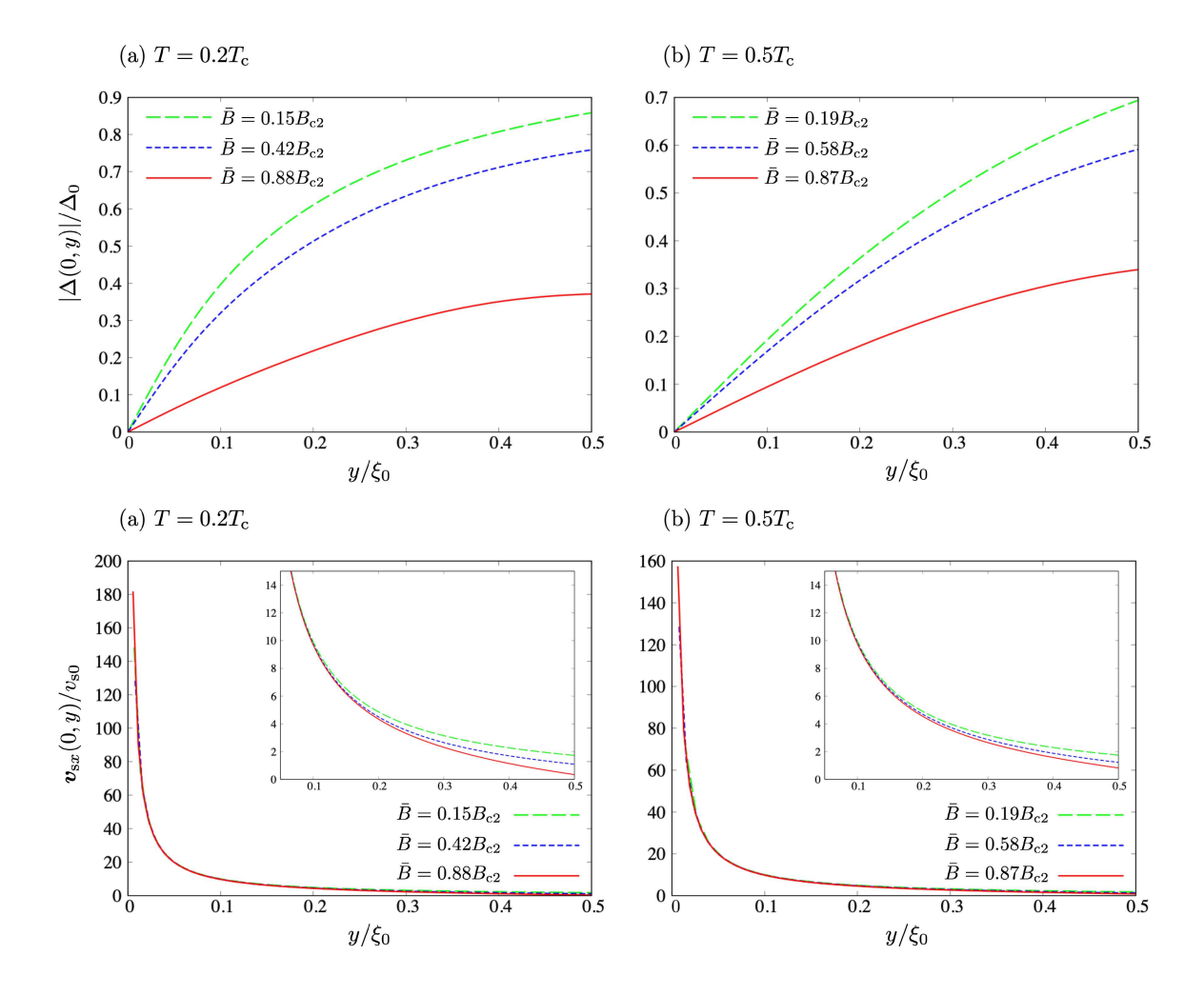


FIG. 6. Gap amplitude $|\Delta(0,y)|$ ((a) and (b)) and the x-component of the superfluid velocity $v_{\rm sx}(0,y)$ ((c) and (d)) on y-axis in units of Δ_0 and $v_{\rm s0} \equiv \Delta_0/mv_{\rm F}$ over $0 \le y \le 0.5\xi_0$ for temperatures $T=0.2T_{\rm c}$ and the average flux densities $\bar{B}=0.15B_{\rm c2}$, $0.42B_{\rm c2}$, and $0.88B_{\rm c2}$, and for temperature $0.5T_{\rm c}$ and the average flux densities $\bar{B}=0.19B_{\rm c2}$, $0.58B_{\rm c2}$, and $0.87B_{\rm c2}$, respectively. Insets are zoomed-in plots.

and by the Lorentz force near the upper critical field. We have also found that low temperatures and magnetic fields about half the upper critical field are suitable for the experimental measurement of electric charge in the vortex core. Moreover, we have shown that the PPG force does not work in equilibrium homogeneous superconductors and even within the Doppler shift method. Therefore, we again emphasize that only the Lorentz force acts on supercurrents away from the isolated vortex core and the Lorentz force may also be important for transport phenomena in the vortex state [20, 45].

There still remains many interesting problems in relation to the study of vortex lattice systems using the AQC equations. For example, our present method can be used to study the flux-flow Hall effect in the vortex lattice by combing the AC response theory based on the standard Eilenberger equations [10, 11], and to also calculate the vortex lattice in ³He [46–50].

Kumagai et al. estimated the vortex-core charge in cuprate superconductors by the NMR/NQR measure-

ments. Although they used the local electric field gradient obtained from changes in the nuclear quadrupole resonance frequency to estimate the vortex-core charge experimentally. To the best of our knowledge, direct observation of the vortex-core charge such as the atomic force microscopy measurement has not been achieved yet. We hope that our present study will stimulate more detailed experiments on vortex-core charging.

ACKNOWLEDGMENTS

We thank T. Uchihashi, J. Goryo, R. C. Regan, A. Kirikoshi, and E. S. Joshua for useful discussions and comments. H.U. is supported in part by JSPS KAK-ENHI Grant No. 15H05885 (J-Physics). The computation in this work was carried out using the facilities of the Supercomputer Center, the Institute for Solid State Physics, the University of Tokyo.

- F. London, Superfluids, Vol. 1 (Dover, New York, 1961)
 p. 56.
- [2] D. I. Khomskii and A. Freimuth, Charged vortices in high temperature superconductors, Phys. Rev. Lett. 75, 1384 (1995).
- [3] G. Blatter, M. Feigel'man, V. Geshkenbein, A. Larkin, and A. van Otterlo, Electrostatics of vortices in type-II superconductors, Phys. Rev. Lett. 77, 566 (1996).
- [4] N. Hayashi, M. Ichioka, and K. Machida, Relation between vortex core charge and vortex bound states, J. Phys. Soc. Jpn. 67, 3368 (1998).
- [5] M. Matsumoto and R. Heeb, Vortex charging effect in a chiral $p_x \pm i p_y$ -wave superconductor, Phys. Rev. B **65**, 014504 (2001).
- [6] M. Machida and T. Koyama, Friedel oscillation in charge profile and position dependent screening around a superconducting vortex core, Phys. Rev. Lett. 90, 077003 (2003).
- [7] T. Kita, Hall coefficient of equilibrium supercurrents flowing inside superconductors, Phys. Rev. B 79, 024521 (2009).
- [8] D. I. Khomskii and F. V. Kusmartsev, Charge redistribution and properties of high-temperature superconductors, Phys. Rev. B 46, 14245 (1992).
- [9] J. Goryo, Vortex with fractional quantum numbers in a chiral p-wave superconductor, Phys. Rev. B 61, 4222 (2000).
- [10] M. Eschrig, J. A. Sauls, and D. Rainer, Electromagnetic response of a vortex in layered superconductors, Phys. Rev. B 60, 10447 (1999).
- [11] M. Eschrig and J. A. Sauls, Charge dynamics of vortex cores in layered chiral triplet superconductors, New J. Phys. 11, 075009 (2009).
- [12] G. E. Volovik, Spontaneous electrical polarization of vortices in superfluid ³He, JETP Lett. **39**, 200 (1984), [Pis'ma Zh. Eksp. Teor. Fiz. **39**, 169 (1984)].
- [13] K.-I. Kumagai, K. Nozaki, and Y. Matsuda, Charged vortices in high-temperature superconductors probed by NMR, Phys. Rev. B 63, 144502 (2001).
- [14] L. P. Gor'kov, Microscopic derivation of the Ginzburg– Landau equations in the theory of superconductivity, Sov. Phys. JETP 9, 1364 (1959), [Zh. Eksp. Teor. Fiz. 36, 1918 (1959)].
- [15] L. P. Gor'kov, Theory of superconducting alloys in a strong magnetic field near the critical temperature, Sov. Phys. JETP 10, 998 (1960), [Zh. Eksp. Teor. Fiz. 37, 1407 (1959)].
- [16] H. Ueki, M. Ohuchi, and T. Kita, Charging in a superconducting vortex due to the three force terms in augmented Eilenberger equations, J. Phys. Soc. Jpn. 87, 044704 (2018).
- [17] T. Kita, Gauge invariance and Hall terms in the quasiclassical equations of superconductivity, Phys. Rev. B 64, 054503 (2001).
- [18] H. Ueki, W. Kohno, and T. Kita, Vortex-core charging due to the Lorentz force in a d-wave superconductor, J. Phys. Soc. Jpn. 85, 064702 (2016).
- [19] N. B. Kopnin, Kinetic equations for clean superconductors: Application to the flux flow Hall effect, J. Low Temp. Phys. 97, 157 (1994).
- [20] E. Arahata and Y. Kato, DC conductivity in an s-wave

- superconducting single vortex system, J. Low Temp. Phys. 175, 345 (2014).
- [21] M. Ohuchi, H. Ueki, and T. Kita, Charging due to pairpotential gradient in vortex of type-II superconductors, J. Phys. Soc. Jpn. 86, 073702 (2017).
- [22] Y. Masaki, Vortex charges and impurity effects based on quasiclassical theory in an s-wave and a chiral p-wave superconductor, Phys. Rev. B 99, 054512 (2019).
- [23] W. Kohno, H. Ueki, and T. Kita, Hall effect in the Abrikosov lattice of type-II superconductors, J. Phys. Soc. Jpn. 85, 083705 (2016).
- [24] W. Kohno, H. Ueki, and T. Kita, Hall effect in the vortex lattice of d-wave superconductors with anisotropic Fermi surfaces, J. Phys. Soc. Jpn. 86, 023702 (2017).
- [25] A. A. Abrikosov, On the magnetic properties of superconductors of the second group, Sov. Phys. JETP 5, 1174 (1957), [Zh. Eksp. Teor. Fiz. 32, 1442 (1957)].
- [26] P. Sharma, Approach to solving quasiclassical equations with gauge invariance, J. Low Temp. Phys. 201, 73 (2020).
- [27] G. Eilenberger, Transformation of Gorkov's equation for type II superconductors into transport-like equations, Z. Phys. 214, 195 (1968).
- [28] T. Kita, Statistical Mechanics of Superconductivity (Springer, Tokyo, 2015).
- [29] J. W. Serene and D. Rainer, The quasiclassical approach to superfluid ³He, Phys. Rep. 101, 221 (1983).
- [30] A. I. Larkin and Y. N. Ovchinnikov, Sign change of the flux-flow Hall effect in HTSC, Vol. 12 (Elsevier, Amsterdam, 1986) p. 493.
- [31] N. B. Kopnin, Theory of Nonequilibrium Superconductivity (Oxford University Press, New York, 2001).
- [32] S. N. Artemenko and A. F. Volkov, Electric fields and collective oscillations in superconductors, Sov. Phys. Usp. 22, 295 (1979).
- [33] E. S. Joshua, H. Ueki, W. Kohno, and T. Kita, Zero-field surface charge due to the gap suppression in d-wave superconductors, J. Phys. Soc. Jpn. 89, 104702 (2020).
- [34] C. Caroli, P. de Gennes, and J. Matricon, Bound fermion states on a vortex line in a type II superconductor, Phys. Lett. 9, 307 (1964).
- [35] K. Yosida, Paramagnetic susceptibility in superconductors, Phys. Rev. 110, 769 (1958).
- [36] U. Klein, Microscopic calculations on the vortex state of type II superconductors, J. Low Temp. Phys. 69, 1 (1987).
- [37] T. Kita, Solving the Ginzburg-Landau equations with magnetic translation group, J. Phys. Soc. Jpn. 67, 2067 (1998).
- [38] M. Ichioka, N. Hayashi, and K. Machida, Local density of states in the vortex lattice in a type-II superconductor, Phys. Rev. B 55, 6565 (1997).
- [39] Y. Nagato, K. Nagai, and J. Hara, Theory of the Andreev reflection and the density of states in proximity contact normal-superconducting infinite double-layer, J. Low Temp. Phys. 93, 33 (1993).
- [40] N. Schopohl and K. Maki, Quasiparticle spectrum around a vortex line in a d-wave superconductor, Phys. Rev. B **52**, 490 (1995).
- [41] N. Schopohl, Transformation of the Eilenberger equations of superconductivity to a scalar Riccati equation,

- e-print arXiv:cond-mat/9804064 (1998).
- [42] E. Helfand and N. R. Werthamer, Temperature and purity dependence of the superconducting critical field, H_{c2} , Phys. Rev. Lett. **13**, 686 (1964).
- [43] T. Kita and M. Arai, Ab initio calculations of $H_{\rm c2}$ in type-II superconductors: Basic formalism and model calculations, Phys. Rev. B **70**, 224522 (2004).
- [44] H. L. Edwards, J. T. Markert, and A. L. de Lozanne, Energy gap and surface structure of YBa₂Cu₃O_{7-x} probed by scanning tunneling microscopy, Phys. Rev. Lett. 69, 2967 (1992).
- [45] H. Ueki, H. Morita, M. Ohuchi, and T. Kita, Drastic enhancement of the thermal Hall angle in a d-wave superconductor, Phys. Rev. B 101, 184518 (2020).

- [46] M. M. Salomaa and G. E. Volovik, Vortices with ferromagnetic superfluid core in ³He-B, Phys. Rev. Lett. 51, 2040 (1983).
- [47] E. V. Thuneberg, Identification of vortices in superfluid ³He-*B*, Phys. Rev. Lett. **56**, 359 (1986).
- [48] T. Kita, Vortex-lattice phases of superfluid ³He in rapid rotation, Phys. Rev. Lett. 86, 834 (2001).
- [49] T. Kita, Unconventional vortices and phase transitions in rapidly rotating superfluid ³He, Phys. Rev. B 66, 224515 (2002).
- [50] R. C. Regan, J. J. Wiman, and J. A. Sauls, Vortex phase diagram of rotating superfluid ³He-B, Phys. Rev. B 101, 024517 (2020).